

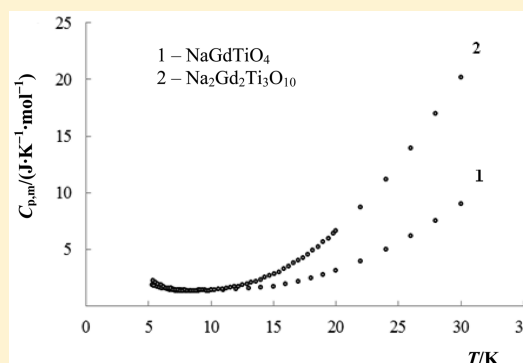
Heat Capacity and Standard Thermodynamic Functions of NaGdTiO_4 and $\text{Na}_2\text{Gd}_2\text{Ti}_3\text{O}_{10}$ over the Range from (6 to 630) K

Alexey V. Markin,^{*,†} Anna M. Sankovich,^{†,‡} Natalia N. Smirnova,[†] and Irina A. Zvereva[‡]

[†]Lobachevsky State University of Nizhni Novgorod, 23/5 Gagarin Avenue, 603950, Nizhni Novgorod, Russia

[‡]St. Petersburg State University, 26 Universitetsky Avenue, Petrodvorets, 198504, St. Petersburg, Russia

ABSTRACT: The heat capacities of layered perovskite-like oxides NaGdTiO_4 and $\text{Na}_2\text{Gd}_2\text{Ti}_3\text{O}_{10}$ were measured by precision adiabatic vacuum calorimetry over the temperature range from $T = (6 \text{ to } 344) \text{ K}$ and by differential scanning calorimetry over the temperature range from $T = (320 \text{ to } 630) \text{ K}$. The standard thermodynamic functions: molar heat capacity $C_{p,m}^\circ$, enthalpy $H^\circ(T) - H^\circ(5)$, entropy $S^\circ(T) - S^\circ(5)$, and Gibbs energy of the compounds were evaluated from the experimental heat capacity temperature dependences over the range from $T = (5 \text{ to } 630) \text{ K}$.



INTRODUCTION

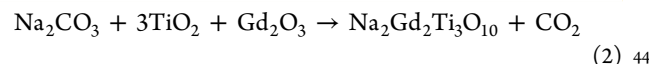
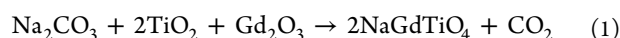
Layered perovskite-like oxides are the objects of close attention because they are one of the promising classes of ceramic materials. Compounds with this crystal structure exhibit remarkable physicochemical properties, such as very large magnetoresistance,¹ multiferroism,² high-temperature superconductivity,³ catalytic and photocatalytic activity,^{4–6} and ion exchange properties.⁷

The knowledge of thermophysical properties for these materials would facilitate their practical application in various branches of chemical engineering and electronics. Moreover, it would be valuable from the theoretical point of view. However, high-quality thermodynamic data available in the literature^{8–11} for this class of compounds are scarce.

The purpose of the present paper is to report the results of calorimetric investigation of layered perovskite-like titanates NaGdTiO_4 and $\text{Na}_2\text{Gd}_2\text{Ti}_3\text{O}_{10}$ over the temperature range from $T = (6 \text{ to } 630) \text{ K}$. These oxides belong to the Ruddlesden–Popper phases¹² $(\text{Na,Gd})_{n+1}\text{Ti}_n\text{O}_{3n+1}$, where n is a number of perovskite layers. Interest in the above oxides is motivated by their use as catalysts for photoinduced reactions and precursors for synthesis of other layered compounds via ion exchange and topochemical routes.¹³

EXPERIMENTAL SECTION

Synthesis and Characterization of Layered Perovskite-like Oxides. The layered perovskite-like oxides NaGdTiO_4 and $\text{Na}_2\text{Gd}_2\text{Ti}_3\text{O}_{10}$ were obtained according to the conventional ceramic technology¹⁴ through the reactions:



The following reactants (Johnson Matthey) were used as the initial compounds: gadolinium oxide Gd_2O_3 (the content of the main component was 99.95 %) preliminarily calcined at $T = 1173 \text{ K}$ for 5 h in order to remove moisture, finely dispersed titanium oxide TiO_2 (99.9 %) in the anatase modification, and sodium carbonate Na_2CO_3 (99.5 %). The reactants were carefully mixed in an agate mortar (on the basis of 40 min of grinding per gram of the initial mixture). The prepared batch mixture was pressed into pellets of 0.5 g in weight and 0.7 cm in diameter. The samples were sintered in a Nabertherm HTCT 01/16 high-temperature furnace in corundum crucibles at atmospheric pressure in air. The temperature conditions were controlled by a platinum–rhodium thermocouple. The isothermal conditions of heat treatment were ensured to be standard uncertainty for temperature $u(T) = 1 \text{ K}$ with the use of a TP-403 programmable temperature controller. NaGdTiO_4 was synthesized at temperature $T = 1073 \text{ K}$ for 4 h, $\text{Na}_2\text{Gd}_2\text{Ti}_3\text{O}_{10}$, at $T = 1273 \text{ K}$ for 10 h.

Characterization of the samples was provided by X-ray powder diffraction analysis and optical emission spectrometry analysis. Qualitative X-ray powder diffraction analysis of the samples was performed on a Rigaku MiniFlex II diffractometer (Cu $K\alpha$ radiation). The XRD patterns (Figure 1) were recorded under the following conditions: $2\theta = 5^\circ$ to 60° at a step of 0.02° and a rate of 2° per min. The phase composition of the samples was determined using the ICDD PDF-2 Database. Optical emission spectrometer ICPE-9000 (Shimadzu, Japan) was used to determine qualitative composition of the samples. No significant

Received: January 14, 2015

Accepted: October 9, 2015



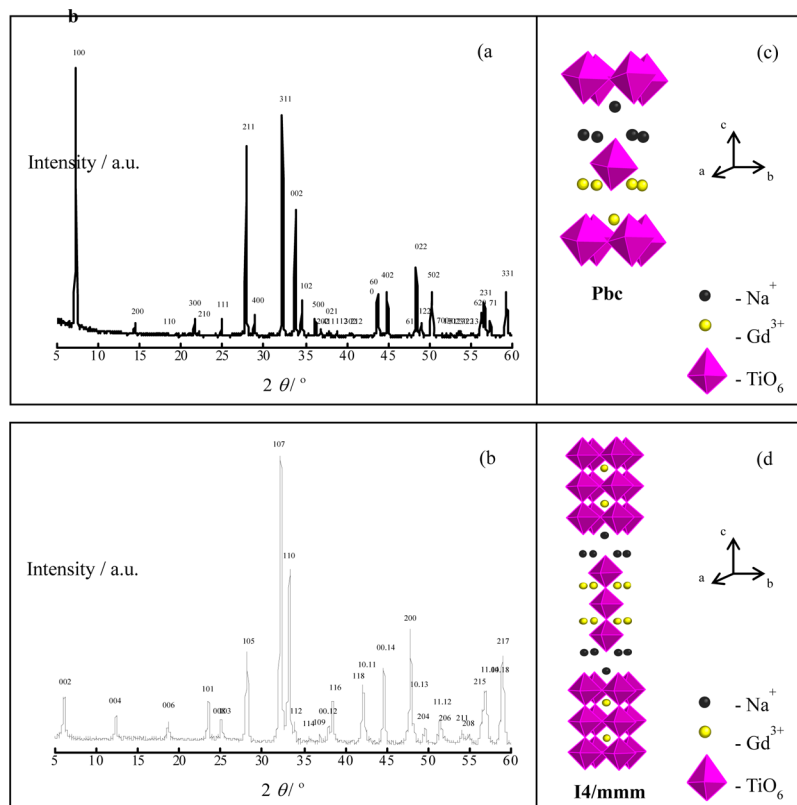


Figure 1. X-ray diffraction patterns of NaGdTlO₄ (a) and Na₂Gd₂Ti₃O₁₀ (b). 2θ is a scattering angle.

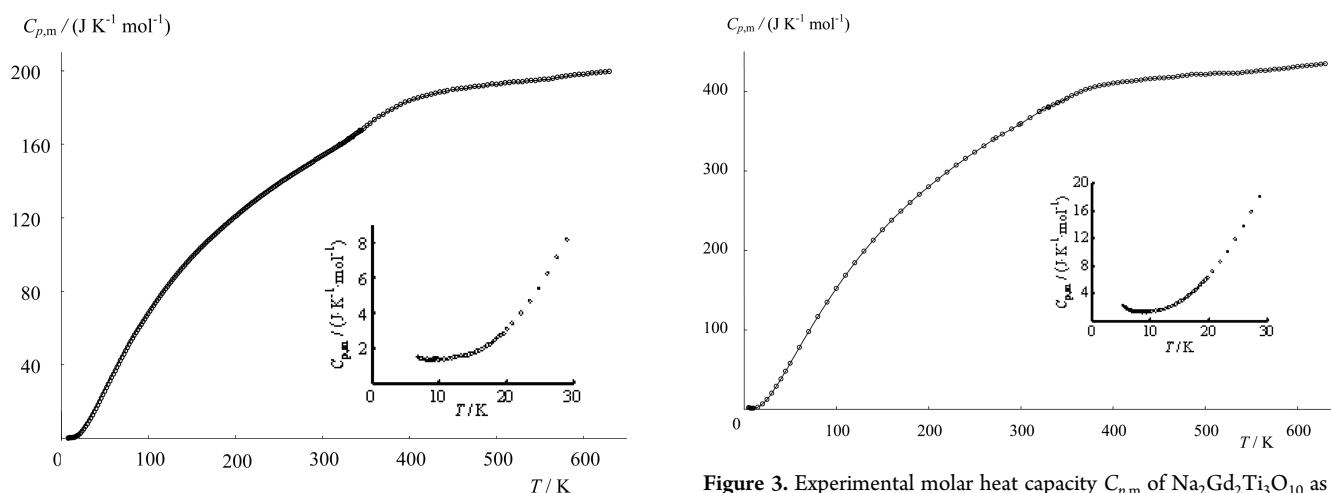


Figure 2. Experimental molar heat capacity $C_{p,m}$ of NaGdTlO₄ as a function of temperature.

Figure 3. Experimental molar heat capacity $C_{p,m}$ of Na₂Gd₂Ti₃O₁₀ as a function of temperature.

impurities were detected, the sensitivity limit is 10^{-9} to 10^{-8} . It is observed that all diffraction peaks match well with the standard data of NaGdTlO₄ (ICDD PDF-2 No. 01-086-0830) or those of Na₂Gd₂Ti₃O₁₀ (ICDD PDF-2 No. 01-086-1372) in our experimental range. No impurity diffraction peaks were found.

The crystal structures of NaGdTlO₄ and Na₂Gd₂Ti₃O₁₀ are displayed in Figure 2 panels c and d, respectively. NaGdTlO₄ belongs to the orthorhombic tetragonal system with the space group *Pbcm* (57) and the symmetry of Na₂Gd₂Ti₃O₁₀ is tetragonal *I4/mmm* (139). It can be seen that the crystal structures consist of single (NaGdTlO₄) or triple (Na₂Gd₂Ti₃O₁₀)

Table 1. Sample Information

chemical name	source	state	mole fraction purity	analysis method
NaGdTlO ₄	present work	powder	0.98	X-ray fluorescence spectrometry, X-ray powder diffraction, optical emission spectrometry, thermogravimetric analysis
Na ₂ Gd ₂ Ti ₃ O ₁₀	present work	powder	0.98	X-ray fluorescence spectrometry, X-ray powder diffraction, optical emission spectrometry, thermogravimetric analysis

Table 2. Experimental Molar Heat Capacity $C_{p,m}$ of Crystalline NaGdTlO₄ ($M = 292.10 \text{ g}\cdot\text{mol}^{-1}$)^a

T	$C_{p,m}$	T	$C_{p,m}$	T	$C_{p,m}$	T	$C_{p,m}$	T	$C_{p,m}$	T	$C_{p,m}$
K	J·K ⁻¹ ·mol ⁻¹	K	J·K ⁻¹ ·mol ⁻¹	K	J·K ⁻¹ ·mol ⁻¹	K	J·K ⁻¹ ·mol ⁻¹	K	J·K ⁻¹ ·mol ⁻¹	K	J·K ⁻¹ ·mol ⁻¹
series 1						series 2					
6.81	1.52	13.62	1.59	34.79	12.79	116.86	80.11	193.72	118.6	270.57	145.3
6.98	1.45	14.00	1.61	36.29	14.04	119.41	81.69	196.28	119.6	273.12	146.0
7.18	1.42	14.38	1.64	37.81	15.37	121.98	83.34	198.84	120.6	275.68	146.8
7.38	1.41	14.76	1.70	39.34	16.74	124.53	84.90	201.40	121.6	278.23	147.5
7.58	1.37	15.15	1.74	40.89	18.06	127.09	86.43	203.95	122.8	280.77	148.2
7.78	1.37	15.52	1.81	42.45	19.50	129.65	87.87	206.51	123.6	283.32	149.0
7.98	1.35	15.92	1.90	44.02	20.95	132.21	89.41	209.07	124.6	285.84	149.8
8.17	1.38	16.31	1.95	45.60	22.45	134.77	90.90	211.63	125.6	288.38	150.5
8.37	1.33	16.71	2.05	47.19	23.92	137.33	92.37	214.19	126.6	290.92	151.2
8.56	1.33	17.11	2.17	48.79	25.45	139.90	93.76	216.75	127.5	294.66	152.0
8.75	1.34	17.51	2.24	50.40	27.01	142.46	95.16	219.31	128.4	297.49	152.5
8.94	1.36	17.92	2.36	52.02	28.57	145.03	96.47	221.87	129.5	300.00	153.9
9.13	1.38	18.33	2.50	53.64	30.04	147.59	97.84	224.44	130.4	302.86	154.4
9.32	1.38	18.74	2.67	55.27	31.51	150.15	99.20	227.00	131.3	306.18	155.4
9.51	1.39	19.17	2.76	56.91	33.04	152.72	100.5	229.56	132.6	309.48	156.3
9.71	1.39	19.59	2.86	58.55	34.55	155.28	101.7	232.13	133.1	312.78	157.3
9.89	1.35	20.01	3.095	60.20	36.04	316.05	158.3	329.14	162.4	342.12	167.3
10.08	1.38	20.85	3.434	61.85	37.52	319.33	159.2	332.40	163.5	345.34	168.7
10.35	1.39	22.13	4.020	63.50	39.02	322.61	160.3	335.65	164.7		
10.70	1.39	23.43	4.694	65.16	40.72	325.88	161.4	338.89	166.0		
11.05	1.39	24.77	5.427	66.82	41.92						
11.40	1.42	26.13	6.260	68.49	43.51	320.1	160	425.1	187	530.1	194
11.76	1.44	27.52	7.200	70.16	45.10	325.1	161	430.1	188	535.1	195
12.12	1.50	28.93	8.195	72.24	46.90	330.1	163	435.1	188	540.1	195
12.49	1.53	30.36	9.286	74.73	49.06	335.1	164	440.1	189	545.1	195
12.86	1.55	31.82	10.43	77.23	51.29	343.1	168	443.8	189	550.1	195
13.24	1.57	33.30	11.59	79.74	53.31	348.1	169	450.1	190	555.1	195
						351.3	170	455.1	190	560.1	195
80.89	53.93	157.85	103.0	234.70	133.9	355.1	172	460.1	190	565.1	196
83.89	56.40	160.41	104.2	237.26	134.7	360.1	173	465.1	191	570.1	196
86.41	58.39	162.98	105.4	239.82	135.7	365.1	175	470.1	191	575.1	197
88.93	60.35	165.54	106.6	242.39	136.5	370.1	176	475.1	192	580.1	197
91.45	62.32	168.11	107.7	244.95	137.4	375.1	178	480.1	192	585.1	197
93.98	64.24	170.67	108.8	247.51	138.2	380.1	179	485.1	192	590.1	198
96.51	66.14	173.24	110.0	250.08	139.1	385.1	180	490.1	192	595.1	198
99.05	67.93	175.80	111.3	252.64	139.8	390.1	182	495.1	193	600.1	198
101.59	69.81	178.36	112.2	255.21	140.7	395.1	183	500.1	193	605.1	198
104.12	71.60	180.93	113.2	257.77	141.4	400.1	184	505.1	193	610.1	199
106.67	73.34	183.49	114.4	260.33	142.2	405.1	185	510.1	193	615.1	199
109.21	75.05	186.05	115.5	262.89	143.0	410.1	185	515.1	194	620.1	199
111.76	76.80	188.60	116.6	265.45	143.7	415.1	186	520.1	194	625.1	199
114.31	78.47	191.16	117.5	268.01	144.5	420.1	187	525.1	194	630.1	199

^aThe standard uncertainty for temperature $u(T) = 0.01 \text{ K}$ in the temperature range from $T = (6 \text{ to } 350) \text{ K}$, and $u(T) = 0.5 \text{ K}$ in the interval between $T = (320 \text{ and } 630) \text{ K}$. The relative standard uncertainty for heat capacity $u_r(C_{p,m}) = 0.02$ in the temperature range from $T = (6 \text{ to } 15) \text{ K}$, $u_r(C_{p,m}) = 0.005$ between $T = (15 \text{ to } 40) \text{ K}$, $u_r(C_{p,m}) = 0.002$ in the temperature range from $T = (40 \text{ to } 350) \text{ K}$, and $u_r(C_{p,m}) = 0.02$ over the range from $T = (320 \text{ to } 630) \text{ K}$.

83 perovskite-like slab layers stacked along the [001] direction
84 which are separated by the rock-salt type double layers. The last
85 are presented by (NaO) and (GdO) layers in the case of
86 NaGdTlO₄ and (NaO) layer for Na₂Gd₂Ti₃O₁₀.

87 The chemical analysis of the investigated titanates was carried
88 out on the energy dispersive X-ray fluorescence spectrometer
89 EDX-900HS (Shimadzu, Japan). From the experimental data it
90 was found that the ratio of elements Ti/Gd is equal to 0.98:1.02,
91 and 2.99:2.01 for NaGdTlO₄ and Na₂Gd₂Ti₃O₁₀, respectively.
92 Additionally, the obtained results allow excluding nonstoichio-
93 metric oxygen in the studied samples.

According to the thermogravimetric (TG) analysis carried out 94
by us, it was established that the samples were thermally stable in 95
the studied temperature range (until $T = 673 \text{ K}$). 96

The information for the studied titanates is listed in Table 1. 97

The molar masses of NaGdTlO₄ and Na₂Gd₂Ti₃O₁₀ were 98
calculated from the International Union of Pure and Applied 99
Chemistry (IUPAC) table of atomic weights.¹⁵ 100

Adiabatic Calorimetry. A BCT precision automatic 101
adiabatic calorimeter (Termis, Moscow) was used to measure 102
isobaric heat capacities ($C_{p,m}$) of NaGdTlO₄ and Na₂Gd₂Ti₃O₁₀ 103
over the temperature range of (6 to 350) K. The design and 104

Table 3. Experimental Molar Heat Capacity $C_{p,m}$ of Crystalline $\text{Na}_2\text{Gd}_2\text{Ti}_3\text{O}_{10}$ ($M = 664.07 \text{ g}\cdot\text{mol}^{-1}$)^a

T K	$C_{p,m}$ $\text{J}\cdot\text{K}^{-1}\cdot\text{mol}^{-1}$	T K	$C_{p,m}$ $\text{J}\cdot\text{K}^{-1}\cdot\text{mol}^{-1}$	T K	$C_{p,m}$ $\text{J}\cdot\text{K}^{-1}\cdot\text{mol}^{-1}$	T K	$C_{p,m}$ $\text{J}\cdot\text{K}^{-1}\cdot\text{mol}^{-1}$	T K	$C_{p,m}$ $\text{J}\cdot\text{K}^{-1}\cdot\text{mol}^{-1}$	T K	$C_{p,m}$ $\text{J}\cdot\text{K}^{-1}\cdot\text{mol}^{-1}$
series 1						series 2					
5.36	2.20	10.91	1.50	24.53	11.90	112.32	172.2	182.08	262.3	252.68	326.0
5.56	2.09	11.23	1.52	25.89	13.76	114.88	176.3	184.67	265.0	255.31	328.0
5.78	1.96	11.53	1.62	27.28	15.85	117.44	180.2	187.27	267.6	257.95	330.0
5.99	1.85	11.86	1.67	28.70	18.07	120.01	184.2	189.87	270.2	260.58	332.2
6.20	1.69	12.20	1.73	30.14	20.52	122.59	188.1	192.47	272.6	263.21	334.1
6.41	1.57	12.54	1.85	31.60	22.94	125.16	192.0	195.06	275.2	265.85	336.0
6.60	1.52	12.89	1.95	33.07	25.59	127.74	195.7	197.66	277.9	268.48	338.1
6.79	1.53	13.24	2.05	34.57	28.21	130.31	199.4	200.26	280.4	271.12	339.9
6.99	1.44	13.60	2.17	36.08	30.88	132.89	203.1	202.87	282.7	273.75	341.7
7.18	1.41	13.96	2.28	37.61	33.70	135.46	206.7	205.49	285.4	276.38	343.7
7.36	1.38	14.32	2.49	39.16	36.60	138.04	210.3	208.10	287.7	279.02	345.8
7.55	1.36	14.68	2.67	40.71	39.57	140.62	213.8	210.71	290.1	281.65	347.3
7.73	1.33	15.06	2.84	42.28	42.56	143.20	217.3	213.32	292.4	284.28	349.1
7.91	1.38	15.43	2.98	43.85	45.69	145.78	220.6	215.93	295.0	286.90	351.1
8.09	1.36	15.81	3.24	45.44	48.89	148.37	223.9	218.54	297.2	289.55	353.1
8.27	1.34	16.19	3.49	47.04	52.01	149.91	227.2	221.15	299.4	292.20	355.1
8.45	1.35	16.58	3.76	48.65	55.29	151.46	230.5	223.76	301.6	294.75	357.1
8.63	1.31	16.97	4.04	50.27	58.63	153.01	233.8	226.37	303.8	297.30	359.1
8.81	1.34	17.35	4.26	51.89	61.81	154.56	237.1	228.98	306.0	299.85	361.1
8.98	1.37	17.75	4.56	53.52	65.10	156.11	240.4	231.59	308.2	302.40	363.1
9.16	1.37	18.15	4.88	55.16	68.18	157.66	243.7	234.20	310.4	304.95	365.1
9.33	1.32	18.56	5.31	56.80	71.45	159.21	247.0	236.81	312.6	307.50	367.1
9.50	1.37	18.97	5.62	58.45	74.83	160.76	250.3	239.42	314.8	310.05	369.1
9.67	1.40	19.39	5.98	60.10	78.20	162.31	253.6	242.03	317.0	312.60	371.1
9.84	1.47	19.81	6.31	61.76	81.39	163.86	256.9	244.64	319.2	315.15	373.1
10.02	1.48	20.63	7.250	63.42	84.61	165.41	260.2	247.25	321.4	317.70	375.1
10.27	1.42	21.89	8.595	65.09	87.97	166.96	263.5	249.86	323.6	320.25	377.1
10.59	1.48	23.20	10.12	66.75	91.38	168.51	266.8	252.47	325.8	322.80	379.1
68.43	94.41	72.19	101.9	77.19	111.5	169.96	269.9	254.98	327.9	325.35	381.1
70.10	97.88	74.69	106.7	79.71	116.1	171.51	273.2	257.59	330.1	327.90	383.1
series 2						DSC					
81.46	119.0	150.95	227.2	221.16	299.5	320.3	375	425.3	414	530.3	423
84.37	124.7	153.54	230.3	223.77	301.8	325.3	378	430.3	414	535.3	423
86.89	129.3	156.13	233.6	226.39	304.0	330.3	380	435.3	416	540.3	424
89.41	133.8	158.72	236.7	229.01	306.9	335.3	383	440.3	416	545.3	425
91.94	138.2	161.31	239.7	231.63	308.9	340.3	386	445.3	416	550.3	425
94.48	142.6	163.92	242.6	234.25	310.7	345.3	388	450.3	417	555.3	426
97.02	147.1	166.51	245.5	236.88	312.8	350.3	391	455.3	417	560.3	426
99.56	151.4	169.10	248.4	239.50	315.0	355.3	395	460.3	418	565.3	426
102.11	155.8	171.70	251.3	242.13	317.4	360.3	397	465.3	418	570.3	427
104.65	160.0	174.29	254.0	244.76	319.6	365.3	400	470.3	419	575.3	428
107.21	164.1	176.88	256.9	247.42	321.8	370.3	403	475.3	420	580.3	428
109.76	168.2	179.48	259.6	250.05	323.8	375.3	404	480.3	420	585.3	429
						380.3	406	485.3	422	590.3	429
						385.3	407	490.3	422	595.3	430
						390.3	408	495.3	422	600.3	431
						395.3	409	500.3	421	605.3	432
						400.3	411	505.3	422	610.3	433
						405.3	411	510.3	423	615.3	433
						410.3	412	515.3	423	620.3	434
						415.3	412	520.3	423	625.3	434
						420.3	413	525.3	423	630.3	435

^aThe standard uncertainty for temperature $u(T) = 0.01 \text{ K}$ in the temperature range from $T = (5 \text{ to } 344) \text{ K}$, and $u(T) = 0.5 \text{ K}$ in the interval between $T = (320 \text{ and } 630) \text{ K}$. The relative standard uncertainty for heat capacity $u_r(C_{p,m}) = 0.02$ in the temperature range from $T = (6 \text{ to } 15) \text{ K}$, $u_r(C_{p,m}) = 0.005$ between $T = (15 \text{ to } 40) \text{ K}$, $u_r(C_{p,m}) = 0.002$ in the temperature range from $T = (40 \text{ to } 350) \text{ K}$, and $u_r(C_{p,m}) = 0.02$ over the range from $T = (320 \text{ to } 630) \text{ K}$.

operation of the calorimeter were described in detail earlier.^{16,17}
 The relative uncertainties in heat capacity measurements were
 $u_r(C_{p,m}) = 0.02$ at $T < 15 \text{ K}$, $u_r(C_{p,m}) = 0.005$ over the tem-
 perature range of $(15 \text{ to } 40) \text{ K}$, and $u_r(C_{p,m}) = 0.002$ between
 $T = (40 \text{ to } 350) \text{ K}$. The accuracy of the calorimeter was verified
 using standard reference samples (benzoic acid and $\alpha\text{-Al}_2\text{O}_3$).
 A titanium calorimetric cell with a volume of 1.5 cm^3 was
 loaded with a sample and then degassed in vacuum with a
 residual pressure of $\sim 5 \text{ Pa}$. Dry helium gas (at $p = 4 \text{ kPa}$ and
 room temperature) was introduced into the cell to facilitate heat
 transfer during the measurements. The sample masses used for

calorimetric measurements were 1.3814 g of NaGdTiO_4 and
 1.6506 g of $\text{Na}_2\text{Gd}_2\text{Ti}_3\text{O}_{10}$.

An iron–rhodium resistance thermometer placed on the inner
 surface of the adiabatic shield was used for the temperature
 measurements in the calorimetric experiments. The temperature
 difference between the cell and the shield was determined by a
 differential copper–iron–chromel thermocouple. The sensitivity
 of the thermometric circuit was 10^{-3} K .

After being assembled, the measuring system was cooled in a
 liquid nitrogen bath. If the measurements were performed below
 80 K , a liquid helium bath was used. The samples were cooled to

Table 4. Smoothed Molar Heat Capacity and Thermodynamic Functions of Crystalline NaGdTlO₄ (*M* = 292.10 g·mol^{−1}) at Pressure *p* = 0.1 MPa^a

<i>T</i>	<i>C</i> _{p,m} ^o	[<i>H</i> ^o (<i>T</i>) − <i>H</i> ^o (5)]	[<i>S</i> ^o (<i>T</i>) − <i>S</i> ^o (5)]	− <i>Φ</i> _m ^{o,b}	<i>T</i>	<i>C</i> _{p,m} ^o	[<i>H</i> ^o (<i>T</i>) − <i>H</i> ^o (5)]	[<i>S</i> ^o (<i>T</i>) − <i>S</i> ^o (5)]	− <i>Φ</i> _m ^{o,b}
K	J·K ^{−1} ·mol ^{−1}	kJ·mol ^{−1}	J·K ^{−1} ·mol ^{−1}	kJ·mol ^{−1}	K	J·K ^{−1} ·mol ^{−1}	kJ·mol ^{−1}	J·K ^{−1} ·mol ^{−1}	kJ·mol ^{−1}
5	1.73	0	0	0	300	153.7	26.48	166.4	23.45
10	1.37	0.00720	1.00	0.00288	310	156.5	28.03	171.5	25.14
15	1.70	0.0147	1.62	0.00957	320	159.5	29.61	176.5	26.88
20	3.089	0.02660	2.284	0.01905	330	162.7	31.22	181.5	28.67
25	5.590	0.04830	3.2307	0.03246	340	166.2	32.86	186.4	30.50
30	8.998	0.08350	4.5153	0.05192	350	170	34.5	191	32.4
40	17.28	0.2157	8.2314	0.1136	360	173	36.3	196	34.3
50	26.62	0.4328	13.06	0.2199	370	176	38.0	201	36.3
60	35.85	0.7475	18.74	0.3772	380	179	39.8	206	38.3
70	44.94	1.150	24.94	0.5963	390	182	41.6	210	40.4
80	53.63	1.645	31.52	0.8771	400	184	43.4	215	42.6
90	61.35	2.219	38.29	1.227	410	185	45.3	219	44.7
100	68.62	2.870	45.13	1.643	420	186	47.1	224	46.9
110	75.62	3.591	52.01	2.130	430	188	49.0	228	49.2
120	82.09	4.381	58.86	2.683	440	189	50.9	233	51.5
130	88.14	5.231	65.68	3.307	450	190	52.8	237	53.9
140	93.80	6.142	72.42	3.996	460	190	54.7	241	56.2
150	99.09	7.106	79.07	4.755	470	191	56.6	245	58.7
160	104.0	8.122	85.62	5.578	480	192	58.5	249	61.2
170	108.6	9.184	92.07	6.468	490	192	60.4	253	63.7
180	112.9	10.29	98.40	7.419	500	193	62.3	257	66.2
190	117.1	11.44	104.6	8.435	510	193	64.3	261	68.8
200	121.0	12.63	110.7	9.511	520	194	66.2	265	71.4
210	125.0	13.86	116.7	10.65	530	194	68.1	268	74.1
220	128.7	15.13	122.6	11.84	540	195	70.1	272	76.8
230	132.3	16.44	128.4	13.10	550	195	72.0	276	79.5
240	135.7	17.78	134.1	14.41	560	195	74.0	279	82.3
250	139.0	19.15	139.7	15.78	570	196	75.9	283	85.1
260	142.1	20.56	145.3	17.21	580	197	77.9	286	88.0
270	145.1	21.99	150.7	18.69	590	198	79.9	289	90.8
280	148.1	23.46	156.0	20.22	600	198	81.9	293	93.8
290	150.9	24.95	161.3	21.81	610	199	83.9	296	96.7
298.15	153.2	26.19	165.5	23.14	620	199	85.8	299	99.7
					630	200	87.8	302	103

^aStandard for temperature $u(T) = 0.01$ K in the temperature range from $T = (5 \text{ to } 344)$ K, and $u(T) = 0.5$ K in the interval between $T = (320 \text{ and } 630)$ K. The standard uncertainty for pressure $u(p) = 10$ kPa. Combined expanded uncertainties for the heat capacity $U_c(C_{p,m}^o)$ are 0.02, 0.005, 0.002, and 0.02; the combined expanded uncertainties $U_c[H^o(T) - H^o(5)]$ are 0.022, 0.007, 0.005, and 0.022; $U_c[S^o(T) - S^o(5)]$ are 0.023, 0.008, 0.006, and 0.023; $U_c[\Phi_m^o]$ are 0.03, 0.01, 0.009, and 0.03 in the ranges $6 \leq T/K \leq 15$, $15 \leq T/K \leq 40$, $40 \leq T/K \leq 344$, and $320 \leq T/K \leq 630$, respectively, for 0.95 level of confidence ($k \approx 2$). ^b $\Phi_m^o = [H^o(T) - H^o(5)] - T[S^o(T) - S^o(5)]$.

the temperature of the measurement onset at a rate of 10^{-2} K·s^{−1}. Then the samples were heated with a temperature step of (0.5 to 2) K at a rate of 10^{-2} K·s^{−1}. Sample temperature was recorded after an equilibration period (temperature drift < 10^{-2} K·s^{−1}, approximately 10 min per experimental point).

The ratio of the sample heat capacity to the total (sample + cell) one was between 0.6 to 0.8.

DSC and TG Analysis. Heat capacities of NaGdTlO₄ and Na₂Gd₂Ti₃O₁₀ over the range of (320 to 630) K were measured in a DSC 204 F1 Phoenix differential scanning calorimeter (Netzsch Gerätebau, Germany) with use of a μ -sensor. The calorimeter was calibrated and tested against melting of *n*-heptane, adamantane, indium, tin, bismuth, and zinc. The heat capacity was determined by the “ratio method”, with sapphire used as a standard reference sample. The curves of heat capacities for both titanates were recorded three times at the repeated cooling and heating of each sample. The $C_{p,m}$ values were reproduced within the limits of the experimental error of the method. The technique

for determining the $C_{p,m}$ according to the data of DSC measurements is described in detail in a Netzsch Software Proteus and in refs 18 and 19. The relative standard uncertainty for heat capacities was $u_r(C_{p,m}) = 0.02$. Measurements were carried out in argon atmosphere. Liquid nitrogen was used as a cryogen.

The thermogravimetric analysis of NaGdTlO₄ and Na₂Gd₂Ti₃O₁₀ over the range of (300 to 673) K was done using a TG 209 F1 Iris thermal microbalance (Netzsch Gerätebau, Germany). The thermal microbalance allows fixing the mass change within standard uncertainty $u(m) = 10^{-5}$ g. The measurement was performed with a heating rate of 10 K·min^{−1} in argon atmosphere. The measuring technique of the TG analysis was standard, according to the Netzsch Software Proteus.

RESULTS AND DISCUSSION

Heat Capacity. Experimental heat capacity data for NaGdTlO₄ and Na₂Gd₂Ti₃O₁₀ in the temperature range of (6 to 630) K are plotted in Figures 2 and 3, and given in Tables 2 and 3,

Table 5. Smoothed Molar Heat Capacity and Thermodynamic Functions of Crystalline $\text{Na}_2\text{Gd}_2\text{Ti}_3\text{O}_{10}$ ($M = 664.07 \text{ g}\cdot\text{mol}^{-1}$) at Pressure $p = 0.1 \text{ MPa}^a$

T	$C_{p,m}^\circ$	$[H^\circ(T) - H^\circ(5)]$	$[S^\circ(T) - S^\circ(5)]$	$-\Phi_m^\circ{}^b$
K	$\text{J}\cdot\text{K}^{-1}\cdot\text{mol}^{-1}$	$\text{kJ}\cdot\text{mol}^{-1}$	$\text{J}\cdot\text{K}^{-1}\cdot\text{mol}^{-1}$	$\text{kJ}\cdot\text{mol}^{-1}$
5	2.06	0	0	0
10	1.39	0.00820	1.11	0.00288
15	2.82	0.0173	1.84	0.0103
20	6.652	0.05230	3.525	0.01819
25	12.57	0.08730	5.209	0.042923
30	20.22	0.1893	8.564	0.06762
40	38.27	0.4830	16.69	0.1845
50	57.92	0.9893	27.42	0.3818
60	77.94	1.619	39.36	0.7429
70	97.65	2.594	53.25	1.134
80	116.6	3.569	67.15	1.803
90	134.8	4.915	82.09	2.473
100	152.1	6.262	97.04	3.442
110	168.6	7.947	112.4	4.412
120	184.3	9.631	127.7	5.689
130	199.0	11.62	143.0	6.966
140	212.9	13.61	158.3	8.549
150	225.9	15.87	173.3	10.13
160	238.1	18.12	188.4	12.02
170	249.5	20.62	203.1	13.90
180	260.2	23.11	217.7	16.08
190	270.4	25.81	232.0	18.26
200	280.1	28.52	246.2	20.72
210	289.4	31.41	260.0	23.18
220	298.5	34.30	273.7	25.92
230	307.3	37.38	287.1	28.66
240	315.7	40.45	300.5	31.66
250	323.7	43.69	313.4	34.67
260	331.5	46.92	326.4	37.93
270	339.5	50.31	338.9	41.20
280	346.4	53.71	351.5	44.71
290	352.7	57.24	363.7	48.23
298.15	358.3	60.11	373.6	51.27
300	359.5	60.76	375.8	51.99
310	367.0	64.43	387.7	55.75
320	374.4	68.10	399.5	59.74
330	380.7	71.91	411.1	63.74
340	385.5	75.71	422.6	67.96
350	391.3	79.63	433.8	72.19
360	397	83.5	445	76.6
370	402	87.5	456	81.1
380	406	91.6	467	85.8
390	408	95.6	477	90.5
400	410	99.7	488	95.3
410	412	104	498	100
420	413	108	508	105
430	414	112	517	110
440	416	116	527	116
450	417	120	536	121
460	418	125	545	126
470	419	129	554	132
480	420	133	563	137
490	422	137	572	143
500	421	141	581	149
510	423	146	589	155
520	423	150	597	161
530	423	154	605	167
540	424	158	613	173
550	425	163	621	179

Table 5. continued

T	$C_{p,m}^{\circ}$	$[H^{\circ}(T) - H^{\circ}(S)]$	$[S^{\circ}(T) - S^{\circ}(S)]$	$-\Phi_m^{\circ b}$
K	J·K ⁻¹ ·mol ⁻¹	kJ·mol ⁻¹	J·K ⁻¹ ·mol ⁻¹	kJ·mol ⁻¹
560	426	167	629	185
570	427	171	636	191
580	428	175	643	198
590	429	180	651	204
600	431	184	658	211
610	432	188	665	218
620	434	193	672	224
630	435	197	679	231

^aStandard for temperature $u(T) = 0.01$ K in the temperature range from $T = (5 \text{ to } 344)$ K, and $u(T) = 0.5$ K in the interval between $T = (320 \text{ and } 630)$ K. The standard uncertainty for pressure $u(p) = 10$ kPa. Combined expanded uncertainties for the heat capacity $U_c(C_{p,m}^{\circ})$ are 0.02, 0.005, 0.002, and 0.02; the combined expanded uncertainties $U_c[H^{\circ}(T) - H^{\circ}(S)]$ are 0.022, 0.007, 0.005, and 0.022; $U_c[S^{\circ}(T) - S^{\circ}(S)]$ are 0.023, 0.008, 0.006, and 0.023; $U_c[\Phi_m^{\circ}]$ are 0.03, 0.01, 0.009, and 0.03 in the ranges $6 \leq T/K \leq 15$, $15 \leq T/K \leq 40$, $40 \leq T/K \leq 344$, and $320 \leq T/K \leq 630$, respectively, for 0.95 level of confidence ($k \approx 2$). ^b $\Phi_m^{\circ} = [H^{\circ}(T) - H^{\circ}(S)] - T[S^{\circ}(T) - S^{\circ}(S)]$.

respectively. Heat capacities of the samples rise gradually with temperature increase over the main temperature interval. At the same time, heat capacities of both compounds were found to increase with a temperature decrease in the range of (6 to 8) K for NaGdTlO₄ and (6 to 10) K for Na₂Gd₂Ti₃O₁₀ (insets in Figures 2 and 3).

The experimental points of $C_{p,m}$ were fitted using least-squares method in the temperature range of (20 to 630) K, and the polynomial equation of the temperature dependency of $C_{p,m}$ was the following:

$$C_{p,m} = \sum_{n=0}^k a_n \left(\frac{T}{30} \right)^n \quad (3)$$

where a_i are polynomial coefficients and k is the polynomial degree. The relative standard uncertainty for the heat capacities was $u_r(C_{p,m}) = 0.005$ in the temperature range of (20 to 90) K, $u_r(C_{p,m}) = 0.0025$ between $T = (80 \text{ to } 350)$ K, and $u_r(C_{p,m}) = 0.006$ between $T = (350 \text{ to } 630)$ K.

The low-temperature heat capacities of both complex oxides are found not to obey the Debye's theory. Such anomalies observed in the heat capacity curves are likely to be descending branches for magnetic disorder–order phase transitions,^{9,20} which lie outside the measuring range of the calorimeter. To give the quantitative description for phase transitions under consideration, magnetic susceptibility measurements as well as heat capacity determined in an external magnetic field are required. However, according to the earlier heat capacity measurements for NaGdTlO₄ in the range of (0.5 to 40) K,²¹ this compound shows a peak at $T = 1.74$ K originated from magnetic transition. The identical character of temperature dependencies of heat capacities of the two titanates over all studied ranges also points out the similarity of structure of both compounds. Thus, the heat capacity of two titanates reaches the saturation level at the same temperature $T \approx 400$ K. The heat capacity of NaGdTlO₄ and Na₂Gd₂Ti₃O₁₀ coincides within an experimental error of $C_{p,m}$ measurements at $T < 12$ K, since a magnetic component²² provides the main contribution to the total heat capacity in this range.

Standard Thermodynamic Functions. As stated above, the extrapolation of heat capacity down to $T = 0$ K was not performed. For this reason we cannot assume the residual entropy to be zero. Hence, we started to determine standard thermodynamic functions from 5 K. The calculations of $H^{\circ}(T) - H^{\circ}(S)$ and $S^{\circ}(T) - S^{\circ}(S)$ were made by numerical integration of

the curves of heat capacities with respect to T and $\ln T$, respectively (Tables 4 and 5), and Φ_m° was equal to $[H^{\circ}(T) - H^{\circ}(S)] - T[S^{\circ}(T) - S^{\circ}(S)]$. The calculation procedure was described in detail elsewhere.²³

CONCLUSIONS

This work reports heat capacities of crystalline layered perovskite-like oxides NaGdTlO₄ and Na₂Gd₂Ti₃O₁₀ studied over the range of (6 to 630) K. Heat capacity measurements were performed by two different calorimetric methods: precise adiabatic vacuum calorimetry and differential scanning calorimetry. Heat capacity anomalies, which are likely to be associated with magnetic ordering, were observed below 8 K for NaGdTlO₄ and below 10 K for Na₂Gd₂Ti₃O₁₀. The standard thermodynamic functions of both compounds over the range of (5 to 630) K were calculated.

AUTHOR INFORMATION

Corresponding Author

*Fax: +7 831 462 35 59. E-mail: markin@calorimetry-center.ru.

Funding

This work was financially supported by the Russian Foundation for Basic Research (Contract No. 14-33-0676) and the Ministry of Education and Science of the Russian Federation (Contract No. 4.1275.2014/K). Adiabatic measurements were performed in Lobachevsky State University of Nizhni Novgorod. Powder X-ray study was carried out in the X-ray Diffraction Centre of St. Petersburg State University. DSC study was carried out in the Thermogravimetric and Calorimetric Research Centre of St. Petersburg State University.

Notes

The authors declare no competing financial interest.

REFERENCES

- (1) Moritomo, Y.; Asamitsu, A.; Kuwahara, H.; Tokura, Y. Giant magnetoresistance of manganese oxides with a layered perovskite structure. *Nature* **1996**, *380*, 141–144.
- (2) Ramesh, R.; Spaldin, N. A. Multiferroics: progress and prospects in thin films. *Nat. Mater.* **2007**, *6*, 21–29.
- (3) Bednorz, J. G.; Müller, K. A.; Takashige, M. Superconductivity in alkaline earth-substituted La₂CuO_{4-y}. *Science* **1987**, *236*, 73–75.
- (4) Shimizu, K.; Itoh, S.; Hatamachi, T.; Sato, M.; Toda, K. Photocatalytic water splitting on Ni-intercalated Ruddlesden–Popper tantalate H₂La_{2/3}Ta₂O₇. *Chem. Mater.* **2005**, *17*, 5161–5166.

- (5) Machida, M.; Miyazaki, K.; Matsushima, S.; Arai, M. Photocatalytic properties of layered perovskite tantalates $MLnTa_2O_7$ ($M = Cs, Rb, Na$, and H ; $Ln = La, Pr, Nd$, and Sm). *J. Mater. Chem.* **2003**, *13*, 1433–1437.
- (6) Tai, Y. W.; Chen, J. S.; Yang, C. C.; Wan, B. Z. Preparation of nano-gold on $K_2La_2Ti_3O_{10}$ for producing hydrogen from photocatalytic water splitting. *Catal. Today* **2004**, *97*, 95–101.
- (7) Silyukov, O.; Chislov, M.; Burovikhina, A.; Utkina, T.; Zvereva, I. Thermogravimetry study of ion exchange and hydration in layered oxide materials. *J. Therm. Anal. Calorim.* **2012**, *110*, 187–192.
- (8) Kyomen, T.; Itoh, M. Calorimetric and structural studies of $La_{1-x}Y_xAlO_3$ and $Y_{1-x}Lu_xAlO_3$ crystals. *J. Therm. Anal. Calorim.* **2002**, *69*, 813–819.
- (9) Akiyama, K.; Aoyama, H.; Abe, N.; Tojo, T.; Kawaji, H.; Atake, T. Low-temperature thermodynamic properties of $Gd_2SrCo_2O_7$. *J. Therm. Anal. Calorim.* **2005**, *81*, 583–586.
- (10) Zinkevich, M.; Solak, N.; Nitsche, H.; Ahrens, M.; Aldinger, F. Stability and thermodynamic functions of lanthanum nickelates. *J. Alloys Compd.* **2007**, *438*, 92–99.
- (11) Kohut, S. V.; Sankovich, A. M.; Blokhin, A. V.; Zvereva, I. A. Low-temperature heat capacity and thermodynamic properties of layered perovskite-like oxides $NaNdTiO_4$ and $Na_2Nd_2Ti_3O_{10}$. *J. Therm. Anal. Calorim.* **2014**, *115*, 119–126.
- (12) Ruddlesden, S. N.; Popper, P. New compounds of the K_2NiF_4 type. *Acta Crystallogr.* **1957**, *10*, 538–539.
- (13) Abdulaeva, L.; Silyukov, O.; Zvereva, I.; Petrov, Y. Soft chemistry synthesis of complex oxides using protonic form of titanates $HLnTiO_4$ ($Ln = La, Nd$). *Solid State Phenom.* **2012**, *194*, 213–216.
- (14) Zvereva, I. A.; Sankovich, A. M.; Missyul', A. B.; Ugolkov, V. L. Mechanism of formation of the complex oxide $Na_2Nd_2Ti_3O_{10}$. *Glass Phys. Chem.* **2010**, *36*, 209–216.
- (15) Wieser, M. E.; Holden, N.; Coplen, T. B.; Böhlke, J. K.; Berglund, M.; Brand, W. A.; De Bièvre, P.; Gröning, M.; Loss, R. D.; Meija, J.; et al. Atomic Weights of the Elements 2011 (IUPAC Technical Report). *Pure Appl. Chem.* **2013**, *85*, 1047–1078.
- (16) Blokhin, A. V.; Paulechka, Y. U.; Kabo, G. J. Thermodynamic properties of $[C_6mim][NTf_2]$ in the condensed state. *J. Chem. Eng. Data* **2006**, *51*, 1377–1388.
- (17) Varushchenko, R. M.; Druzhinina, A. I.; Sorkin, E. L. Low-temperature heat capacity of 1-bromoperfluorooctane. *J. Chem. Thermodyn.* **1997**, *29*, 623–637.
- (18) Höhne, G. W. H.; Hemminger, W. F.; Flammersheim, H.-J. *Differential Scanning Calorimetry*; Springer-Verlag Berlin Heidelberg: New York, 2003.
- (19) Drebuschak, V. A. Calibration Coefficient of Heat-Flow DSC. Part II. Optimal Calibration Procedure. *J. Therm. Anal. Calorim.* **2005**, *79*, 213–218.
- (20) Missyul, A. B.; Zvereva, I. A.; Palstra, T. T. M.; Kurbakov, A. I. Double-layered Aurivillius-type ferroelectrics with magnetic moments. *Mater. Res. Bull.* **2010**, *45*, 546–550.
- (21) Ozawa, T. C.; Ikoshi, A.; Taniguchi, T.; Mizusaki, S.; Nagata, Y.; Noro, Y.; Samata, H.; Takayanagi, S. Magnetic spin interactions observed by heat capacity measurements for layered compounds: $NaLnTiO_4$ ($Ln = Sm, Eu, Gd, Tb, Dy, Ho$ and Er). *J. Alloys Compd.* **2008**, *448*, 64–68.
- (22) Toda, K.; Kameo, Y.; Kurita, S.; Sato, M. Crystal structure determination and ionic conductivity of layered perovskite compounds $NaLnTiO_4$ ($Ln = rare\ earth$). *J. Alloys Compd.* **1996**, *234*, 19–25.
- (23) McCullough, J. P.; Scott, D. W. *Calorimetry of Non-reacting Systems*; Butterworth: London, 1968; pp 206–207.